Optical and Quantum Electronics 11 (1979) 43–59

Curvature and microbending losses in single-mode optical fibres

W. A. GAMBLING, H. MATSUMURA, C. M. RAGDALE
Department of Electronics, University of Southampton, Southampton, UK

Received 2 August 1978

Curvature of a single-mode optical fibre gives rise to two principal forms of additional transmission loss, namely transition loss and pure bend loss. The transition loss and the associated ray radiation, which have been observed at the beginning of a bend, can be satisfactorily explained by a modified coupled-mode theory. The radiation modes are represented by a quasi-guided mode having an average propagation constant β_e. The introduction of a gradual change of curvature reduces the transition loss much more than the pure bend loss. Analysis of the microbending loss shows that the transition component is a maximum at a given correlation length which can be simply expressed in terms of β_e. The contributions of both transition and bend components to the total microbend loss have been derived for the case of a randomly-curved fibre for several autocorrelation and density functions.

1. Introduction

A consideration of the radiation loss caused by curvature of a single-mode fibre is very important from the point of view of long-distance transmission of optical signals. Several theories on curvature loss have been proposed, most of which assume [1, 2] that the fields at a bend can be approximated by those of a straight fibre. However it has been shown that in propagating from a straight, to a curved, portion of fibre the field distribution changes considerably [3–7]. Thus in addition to a pure bending loss, a redistribution of energy, from that of the straight fibre mode to that of a curved fibre mode, must take place over a finite length at the beginning of a bend and the loss due to mode conversion in this 'transition region' must also be considered. These two different physical phenomena have been isolated and observed separately [8] and it has been found that the mode conversion loss, which we have called the 'transition loss', can predominate at large bend radii.

It is necessary to extend these results to the case of a fibre with an arbitrary curvature distribution. Obviously analysis would be simplified if one type of loss were to predominate. Thus the microbending loss in a single-mode fibre [9, 10] is normally calculated by taking into account only the mode conversion loss from the HE_{11} mode to the radiation modes. It is further assumed that microbending occurs at a relatively large radius of curvature, in which case the transition loss may indeed exceed the bending loss, as it does when the bend radius at the junction between straight and curved sections of fibre changes abruptly. However in a practical situation, the radius of curvature normally changes continuously and slowly because of the mechanical stiffness of the fibre. In addition, the microbend radius could be small and it is therefore not obvious that the assumptions normally made in microbending loss calculations are actually applicable in practice. For example, a very interesting and relevant experimental observation [8] showed recently that the radiation loss of a fibre having a sinusoidal curvature could be accounted for solely in terms of pure bending loss. However we believe that if the periodic length of the sinusoid could be further increased then the transition loss effect might become larger than the pure bending loss, but it was not possible to realise this condition experimentally. The results suggest clearly that any propagation study must take into account the pure bending loss as well as the transition loss.

Another experimental observation [11] shows that the radiation emitted at the beginning of a bend is not continuous but seems to occur in ray form. This behaviour has been considered theoretically in

terms of whispering-gallery modes [12] or of only one leaky mode [13], but so far only qualitative agreement has been obtained with experiment. A first-order perturbation theory [4, 10] applied to the wave equations cannot strictly be used because, in this approximation, the propagation constant of the perturbed field is the same as that of the mode in the straight fibre.

Because of the above anomalies and difficulties we have made a detailed study of propagation in a curved fibre having an arbitrary longitudinal undulation. The transition loss is calculated from a mode-coupling theory. Usually the mode coupling theory [14] can only be applied to the case of small undulation of the fibre axis and we therefore propose a modified coupling coefficient in Section 2 which is used to calculate the transition loss in various types of bend. In Section 3, the pure bend loss is considered, while the contributions of both forms of loss to microbending are considered in Section 4.

2. Transition loss

2.1. Power density in the radiation modes

In a straight step-index fibre with core radius a, refractive index n_1 and having an infinite cladding of index n_2, the propagation constant β of the guided modes is restricted to the interval $n_2k < \beta < n_1k$ where $k = \omega(\mu_0\epsilon_0)^{1/2} = 2\pi/\lambda$ and λ is the wavelength in free space. If, in the usual way, we define parameters

$$\begin{aligned} U^2 &= (kn_1a)^2 - (\beta a)^2 \\ W^2 &= (\beta a)^2 - (kn_2a)^2 \end{aligned} \tag{1}$$

and

$$V^2 = U^2 + W^2 = (ka)^2 (n_1^2 - n_2^2)$$

then the modal fields of the fibre can be completely described. For $V < 2.405$ only the HE_{11} guided mode can propagate in the fibre and to realise this condition the relative index difference Δ defined by $\Delta = (n_1 - n_2)/n_2$ must be small (say 0.05% ~ 0.15%) so that the mode is relatively weakly bound.

In the weak-guidance approximation the electric field can be assumed to be linearly polarized. Moreover the bent fibre may be represented, through a conformal transformation, by an equivalent straight fibre where the influence of curvature is taken into account by introducing an effective refractive-index profile [3]

$$n_e = n_{1,2} [1 + (r/R) \cos\theta] \tag{2}$$

where $n_{1,2}$ is the refractive index in the core, cladding; r, θ are circular coordinates; while R is the radius of curvature of the fibre which is generally a function of fibre length.

As shown in Fig. 1a the curved portion of fibre is terminated at $z = 0, L$ by straight sections. Since a straight fibre with the effective refractive-index distribution n_e of Equation 2 has the same properties as the equivalent bent fibre, the curvature distribution in Fig. 1a can be represented by a straight fibre having a varying refractive-index distribution as illustrated schematically in Fig. 1b.

The transverse electromagnetic fields of a single-mode fibre having the refractive-index distribution of Equation 2 can be expressed by a series expansion in terms of the HE_{11} guided mode plus an integration over radiation modes

$$\begin{aligned} \bar{E}_t &= a_0(z)\bar{e}_0(r, \theta) + \sum \int_0^\infty a_\mu(z)\bar{e}_\mu(r, \theta)\, d\rho \\ \bar{H}_t &= b_0(z)\bar{h}_0(r, \theta) + \sum \int_0^\infty b_\mu(z)\bar{h}_\mu(r, \theta)\, d\rho \end{aligned} \tag{3}$$

where $\bar{e}_\mu, \bar{h}_\mu$ are the transverse modal fields, and $a_\mu(z), b_\mu(z)$ are their z-dependent mode amplitudes; ρ is the parameter concerned with the propagation constant of the radiation modes in the z-direction, see Equation 8. The suffix $\mu = 0$ denotes the HE_{11} guided mode and $\mu \neq 0$ radiation modes. Substitution of Equations 2 and 3 into Maxwell's equation and use of the orthogonality conditions then leads to a system of coupled equations. We assume here that the radius of curvature R is not too small so that there is only weak coupling between the HE_{11} guided mode and the radiation modes. Correspondingly the radiation modes are not instantaneously lost from the core region. With the given boundary con-

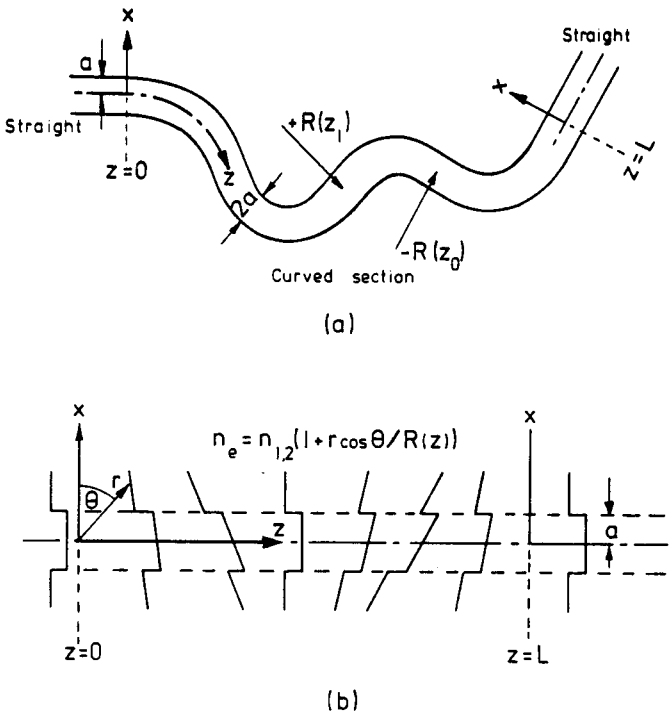

Figure 1 Random bends in a fibre (a) between $z = 0$ and $z = L$ and the equivalent refractive index distribution (b) of a straight fibre.

ditions at the input and output ends of the fibre, namely that at $z = 0$ only the forward HE_{11} mode with power P exists and at $z = L$ all backward waves disappear, then the system of coupled equations can be solved by perturbation theory. The complete set of forward and backward waves can thus be described by

$$\begin{aligned} a_\mu(z) &= C_\mu^+(z)\exp(-j\beta_\mu z) + C_\mu^-(z)\exp(j\beta_\mu z) \\ b_\mu(z) &= C_\mu^+(z)\exp(-j\beta_\mu z) - C_\mu^-(z)\exp(j\beta_\mu z) \end{aligned} \tag{4}$$

where the expansion coefficients of the forward and backward waves are

$$\begin{aligned} C_\mu^+(z) &= C_0^+(0)\int_0^z \frac{K(\beta_\mu)}{R(z)}\exp[j(\beta_\mu - \beta_0)z]\,dz \\ C_\mu^-(z) &= -C_0^+(0)\int_0^z \frac{K(\beta_\mu)}{R(z)}\exp[-j(\beta_\mu + \beta_0)z]\,dz \end{aligned} \tag{5}$$

and β_μ is the propagation constant. The coupling coefficient $K(\beta_\mu)$ between the HE_{11} mode and the radiation mode of order μ is given by

$$K(\beta_\mu) = \frac{\omega\epsilon_0}{j4P}\int_0^{2\pi}\int_0^\infty r^2(\bar{e}_\mu^*\bar{e}_0)\cos\theta\,dr\,d\theta. \tag{6}$$

The contribution of the longitudinal electric field components have been omitted because of the weak-guidance approximation. The coupling coefficient derived in this way is slightly different from that given by the usual mode coupling theory [14] because Equation 6 contains an r^2 term instead of the usual r term.

The next step is to integrate Equation 6. As we are now considering a curved fibre of large bend radius we can expect the radiation to escape at a small angle relative to the fibre axis. Therefore we can assume coupling only to the radiation modes which have propagation constants close to n_2k. Substitution of the field of the HE_{11} guided mode, and of the radiation modes [14], into Equation 6 and use of

the integral formula given in the Appendix then leads to

$$K(\beta_\mu) = \frac{4a^2 knVW\rho^{1/2} J_0(U)J_1(S)}{j\pi(X_0^2 - X^2)^2 |J_1(U)|\,|SJ_0(S)H_1^1(Q) - QJ_1(S)H_0^1(Q)|} \tag{7}$$

where

$$S^2 = (kn_1a)^2 - X^2; \quad Q^2 = (\rho a)^2 = (kn_2a)^2 - X^2; \quad X = \beta a; \quad X_0 = \beta_0 a \tag{8}$$

and functions $J_n(x)$, $H_n^1(x)$ are Bessel and Hankel functions of the first kind. The integration over θ in Equation 6 shows that only the radiation modes having $\mu = \pm 1$ can be coupled to the HE_{11} mode. This important result is identical with that obtained for the multimode fibre some years ago [15]. Finally, the power P_r, contained in the radiation mode at $z = L$ can be calculated by appropriate integration of the Poynting vector. Taking into account the symmetry of the Bessel function for $\mu = \pm 1$, we obtain

$$P_r = 2\frac{L}{a} A(U, W) \int_{-kn_2a}^{kn_2a} B(X)F^2(L, X)\,dX \tag{9}$$

where

$$A(U, W) = [4V^2 WJ_0(U)/\sqrt{(2\Delta)}\pi J_1(U)]^2$$

$$B(X) = \frac{|X|(X_0^2 - X^2)^{-4} J_1^2(S)}{|SJ_0(S)H_1^1(Q) - QJ_1(S)H_0^1(Q)|^2} \tag{10}$$

and

$$F^2(L, X) = \left| \frac{1}{\sqrt{(L/a)}} \int_0^L \frac{1}{R(z)} \exp\left[j(X - X_0)\frac{z}{a} \right] dz \right|^2.$$

In this calculation, the input power of the HE_{11} mode at $z = 0$, i.e. $P|C^+(0)|^2$ has been normalized to 1. The integration over the range of propagation constants is represented by Equation 9 and along the length of curved fibre by the integral in the expression for $F^2(L, X)$ in Equation 10. Thus the total power loss α of the waveguide due to curvature is given by

$$\alpha = -10 \log_{10}(1 - P_r) \sim 4.343 P_r \quad \text{(dB)}. \tag{11}$$

From Equation 9, the power density for the radiation modes is given by

$$\frac{dP_r}{dX} = 2\left(\frac{L}{a}\right) A(U, W)B(X)F^2(L, X). \tag{12}$$

Two important parameters which will be used in the following calculations are now introduced. These are a power-weighted mean value of the propagation constant for the radiation modes ($X_e = \beta_e a$) and the r.m.s. deviation from that mean (σ_r), as defined by [16]

$$X_e = \frac{2(L/a)A(U, W)}{P_r} \int_{-kn_2a}^{kn_2a} XB(X)F^2(L, X)\,dX \tag{13}$$

and

$$\sigma_r^2 = \frac{2(L/a)A(U, W)}{P_r} \int_{-kn_2a}^{kn_2a} (X - X_e)^2 B(X)F^2(L, X)\,dX. \tag{14}$$

Thus X_e is the average propagation constant of the radiation modes while σ_r^2 is the variance of the propagation constants and is a measure of the coherence of the power propagating in the radiation modes. If σ_r^2 is small then the radiation modes behave as a quasi-guided mode having an average propagation constant X_e.

2.2. Transition to constant radius of curvature

The case is now considered where a section of straight fibre carrying the HE_{11} mode is connected to a length of similar fibre curved at a constant bend radius $R(z) = R_0$. At the transition the energy coupled into radiation modes constitutes the loss and will now be calculated. Hitherto most authors have assumed that the change in curvature is instantaneous but in practice this cannot be so because of the

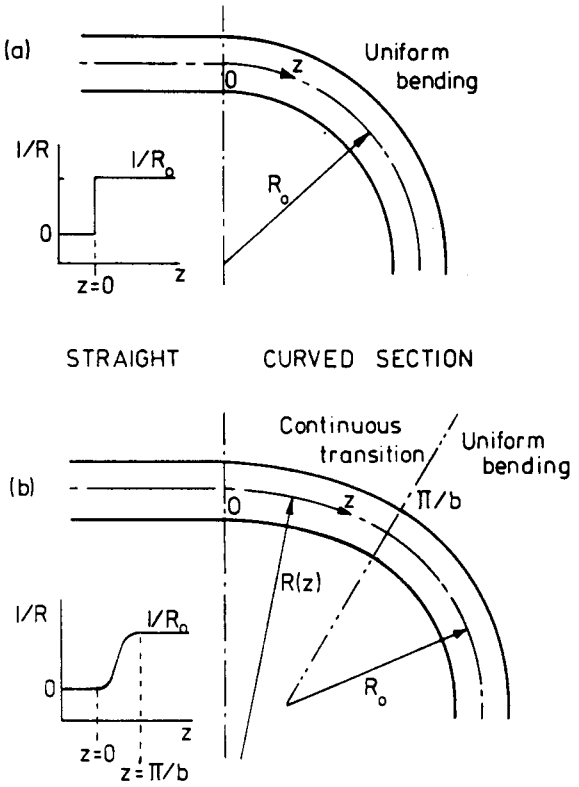

Figure 2 Abrupt (a) and continuous (b) transitions between straight ($R = \infty$) and constantly-curved ($R = R_0$) sections of fibre.

mechanical stiffness of the fibre. The magnitude of the transition loss must obviously depend on the rate of change of curvature [8]. We will therefore consider separately the two cases of (a) an abrupt change and (b) a continuous transition, at the junction, as shown in Fig. 2a and b, respectively.

2.2.1. Abrupt change of curvature

In the case of an abrupt transition $F(L, X)$ in Equation 10 is given by

$$F^2(L,X) = 2\left(\frac{a}{L}\right)\left(\frac{a}{R_0}\right)^2\left\{1-\cos\left[(X-X_0)\frac{L}{a}\right]\right\}/(X-X_0)^2. \qquad (15)$$

Figs. 3a and b show the power density in the radiation modes for $L/a = 20$ and 400, respectively, as a function of the propagation constant. It is found that the radiation power varies non-uniformly with βa, but only those radiation modes having propagation constants close to kn_2a contain any appreciable power. The power density for backward waves is indicated in Fig. 3a by dashed curves, but is too small to be shown in Fig. 3b. Thus scattering is predominantly in the forward direction and the reflected waves can be neglected.

The power in the radiation modes as a function of normalized length can be calculated from Equations 9 and 15. The results for $V = 2.4$ and $\Delta = 0.0005$ are shown in Fig. 4. The radiation power is an oscillatory function of fibre length indicating that in addition to the coupling of power in to the radiation modes, part of the radiation mode power couples back into the HE_{11} guided mode. However a steady state is approached with increase of fibre length. The transmission loss corresponding to the transition loss at two abrupt junctions can be calculated by using Equation 11. It is of interest to make a comparison with existing results which have been obtained theoretically [4, 7, 10] and experimentally [8]. According to the earlier theories the loss is given by the first-order perturbation under the assumption that the power coupled to the radiation modes radiates away from the waveguide and is lost in-

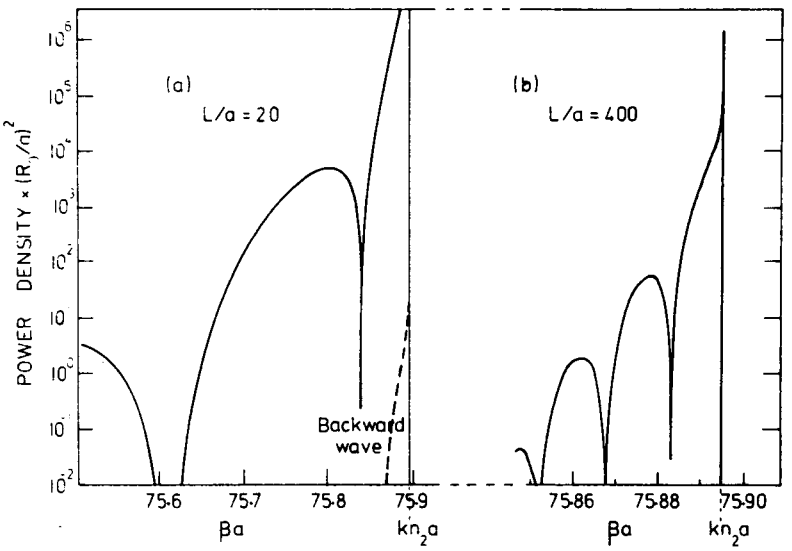

Figure 3 Normalized power density in the radiation modes as a function of βa when $V = 2.4$, $\Delta = 0.05\%$ at normalized lengths (a) $L/a = 20$ and (b) $L/a = 400$. The dashed line represents the power contained in the backward waves.

stantaneously at the junction. The simplest loss formula, derived from [7], is given by

$$\alpha = \frac{1}{(R_0/a)^2}\frac{V^4}{32\Delta^2}(0.65 + 1.62V^{-1.5} + 2.88V^{-6})^6 \qquad (16)$$

and is shown in Fig. 4 by the solid line. The more rigorous value [4] derived by Miyagi and Yip is shown by the dotted line. The results are similar, especially for longer fibre lengths, and seem to be near the average or steady-state value of the oscillating radiation power. Therefore we can infer that Equation 16 only gives the loss in the curved fibre at large distances from the junction. Over shorter lengths, i.e. in the transition region, it is important to consider the contribution of the radiation modes because the considerable amount of power which they contain can be partially coupled back into the guided mode. It follows that if the fibre axis changes direction continuously the portion of this power which is coupled back can have a considerable influence on the transmission loss.

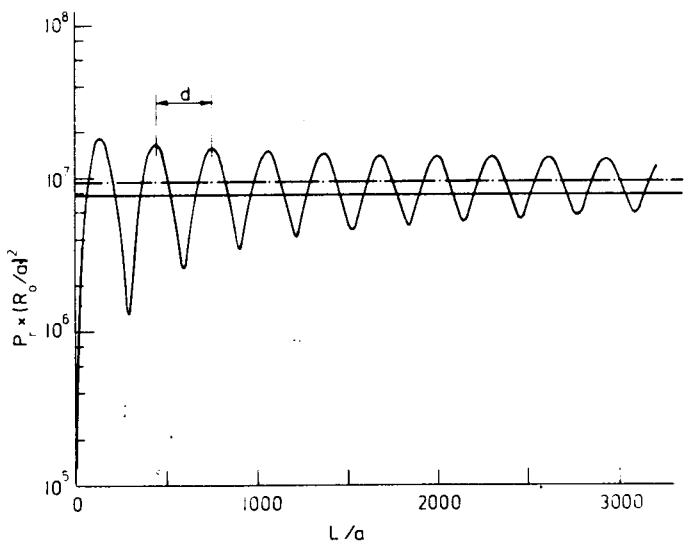

Figure 4 Normalized power in radiation modes along a curved fibre following an abrupt change of curvature for $V = 2.4$ and $\Delta = 0.05\%$. The solid line is obtained from Equation 16 and the dashed line from [4].

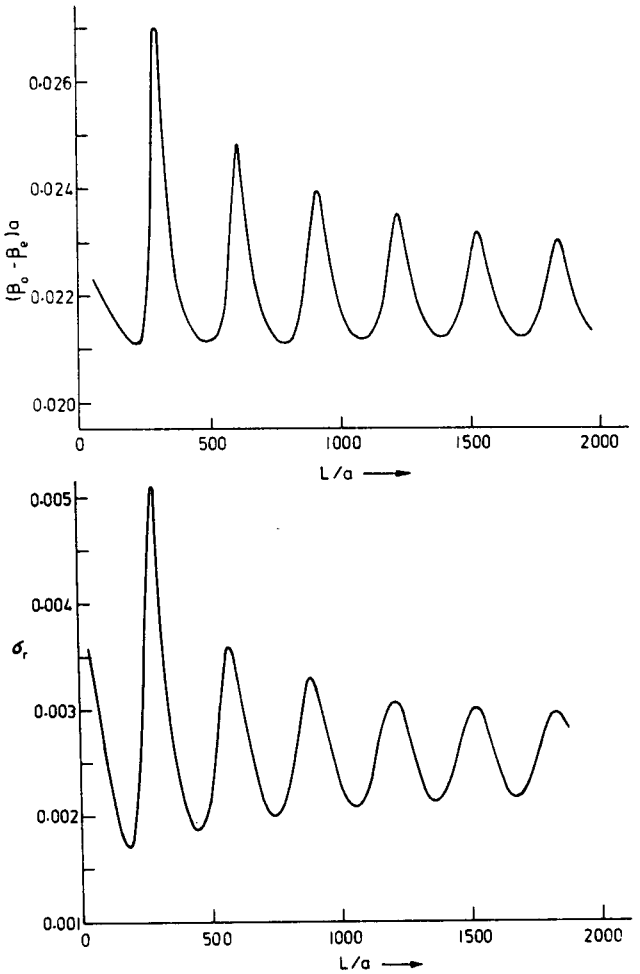

Figure 5 Average propagation constant β_e of the radiation modes (a) and the standard deviation (b) as a function of length for $V = 2.4$ and $\Delta = 0.05\%$.

The average propagation constant of the radiation modes, and the standard deviation, derived from Equations 13 and 14, are shown in Figs. 5a and b, respectively. It can be seen that β_e varies periodically with the fibre length and differs from the propagation constant of the HE_{11} mode, see Fig. 5a, by only about 0.022 in this calculation. The power-weighted r.m.s. deviation, Fig. 5b, is also small which means that there is only a narrow power spectrum of radiation modes.

Comparison of Figs. 4 and 5 indicates that each peak in the radiation power curve of Fig. 4 corresponds to a minimum difference between β_e and β_0 while at the same time the r.m.s. spread of propagation constants in the radiation modes is a minimum. The power transferred from the HE_{11} mode to radiation modes at these points is therefore a maximum. Thus the radiation is approximately coherent at each maximum in the radiated power density so that the various modes emerge in almost the same direction. As a result the radiation emitted at the beginning of the bend occurs preferentially in one direction, in complete agreement with the rays observed experimentally [5, 11].

Sammut [12] has explained the ray radiation in terms of coupling between the HE_{11} and the LP_{11} leaky mode. Here we have shown that when σ_r is small a two-mode coupling theory can again be used because the radiation modes behave as a quasi-guided mode having an average propagation constant β_e. However in other regions this theory may not be applicable.

In order to illustrate more clearly the relation between the power density and the propagation constants, P_r is drawn as a function of βa in Fig. 6 for $V = 2.4$, $\Delta = 0.0005$ and $L/a = 400$. It can be seen

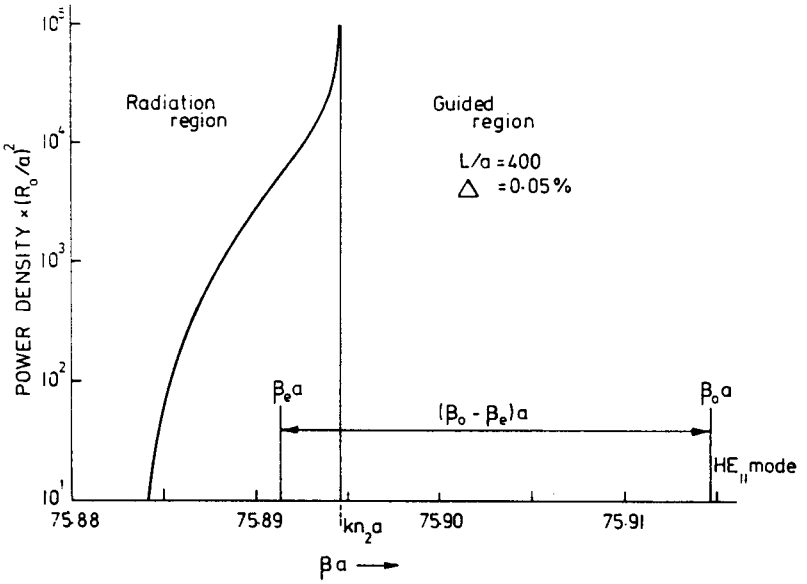

Figure 6 Normalized power density of the radiation modes and the average propagation constant β_e for $V = 2.4$; $\Delta = 0.05\%$; $L/a = 400$.

that the power-weighted average propagation constant β_e for the radiation modes is fairly close to kn_2. The parameter $(\beta_0 - \beta_e)a = X_0 - X_e$ shown in Fig. 6 is a very important one. Because the r.m.s. deviation is small the radiation modes, as we have argued above, act approximately like a single quasi-guided mode with propagation constant β_e. This mode does not actually exist, of course, but it is a useful concept in explaining the phenomena occurring in a curved fibre. We will call this quasi-guided mode the $R(\beta_e)$ mode. In this case, the problem can be simplified by considering coupling between the HE_{11} mode and the $R(\beta_e)$ mode so that the power oscillation can be easily understood [12, 15]. Moreover the normalized oscillation period (d) shown in Fig. 4 may be approximated by

$$d = 2\pi/(X_0 - X_e) = 2\pi/a(\beta_0 - \beta_e) \tag{17}$$

and has a value of about 300. Alternatively Fig. 5a shows that for $\Delta = 0.0005$ and $V = 2.4$, the average of the minima is $X_0 - X_e = 0.0212$ giving $d = 296$. These two results are very close thus supporting the idea of a quasi-guided radiation mode, especially for short lengths of curved fibre.

It is interesting to compare the predictions of the proposed Equation 17 with experimental measurements. Thus Fig. 1 of [5] shows the measured variation of intensity in the plane of the bend at the junction between straight and curved sections of a fibre having a core radius of 4.1 μm, NA (numerical aperture) = 0.06 and $V = 2.38$. The bend radius was 10 mm. In the transition region, where the bend radius is expected to have become reasonably constant, the periodic length, as given by the separation of the intensity peaks, is 0.89 mm. The value derived from Equation 17 is 0.92 mm showing that there is good agreement between this equation, hence the above theory, and experiment.

2.2.2. Continuous transition at the junctions

In practice the radius of curvature of the fibre in the transition region changes continuously at the beginning of the bend before becoming constant. Let us assume, as illustrated in Fig. 2b, that the change in radius of curvature may be described by

$$\begin{aligned} R(z) &= 2R_0(1 - \cos bz)^{-1} && \text{for } 0 \leqslant z \leqslant \pi/b \\ &= R_0 && \text{for } \pi/b \leqslant z \leqslant L - \pi/b \\ &= 2R_0\{1 - \cos[b(L - z)]\}^{-1} && \text{for } L - \pi/b \leqslant z \leqslant L\,. \end{aligned} \tag{18}$$

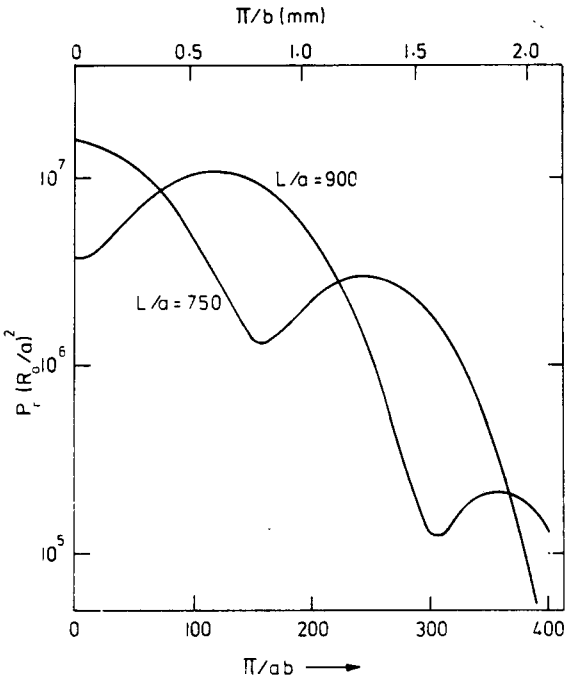

Figure 7 Radiation mode power as a function of the length of region of changing curvature as defined in Equation 18 for $V = 2.4$; $\Delta = 0.05\%$.

At $z = 0, \pi/b, L - \pi/b$ and L we have $d(R^{-1})/dz = 0$ so that $F(L, X)$ in Equation 10 becomes

$$F^2(L,X) = \left(\frac{a}{L}\right)\left(\frac{a}{R_0}\right)^2 \left(\frac{2(ab)^2 \cos\left[(X-X_0)\pi/2ab\right] \sin\left\{\left[(X-X_0)/2\right]\left(L/a - \pi/ab\right)\right\}}{(X-X_0)^2\left[(ab)^2 - (X-X_0)^2\right]}\right)^2. \tag{19}$$

The normalized length of the region of changing curvature is π/ab.

The power contained in the radiation modes can be obtained from Equations 9 and 19 and is shown in Fig. 7 as a function of π/ab for $L/a = 750$ and 900, with $V = 2.4$ and $\Delta = 0.0005$. The two curves correspond approximately to the peak and the valley of the oscillation in Fig. 4. The top scale shows the actual length of the changing-curvature region (i.e. π/b). The limiting case $\pi/ab = 0$ corresponds to an abrupt change of curvature. As before, the power in the radiation modes varies periodically with distance but with increase of π/ab it, and hence the radiation loss, decreases rapidly. For example with $\pi/ab = 400$, corresponding to a changing-curvature length of 2.1 mm, the radiation power is two orders smaller than in the case of an abrupt change. The calculations indicate that the transition loss is very small if the fibre curvature changes gradually.

3. Pure bend loss

We have so far only considered the transition loss, but the pure bend loss, as in a uniformly bent fibre, also has to be taken into account. Marcatili and Miller [17] have explained this phenomenon as follows. With increasing distance from the centre of curvature the local phase velocity must increase. At a certain distance it reaches the limiting velocity of light and the fraction of the mode field beyond this point is no longer guided and radiates away from the fibre. The pure bend loss in a fibre of length L and having a varying radius of curvature $R(z)$ may be expressed as [8]

$$\alpha_b = \int_0^L \frac{C(U,W)}{\sqrt{|R(z)|}} \exp\left\{-D(U,W)|R(z)|\right\} dz \tag{20}$$

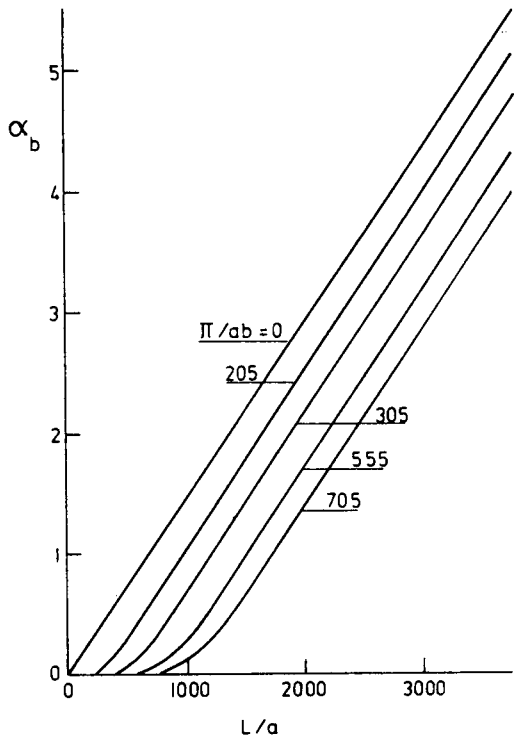

Figure 8 Variation of pure bend loss with length for various rates of change of curvature for $R_0/a = 6000$; $V = 2.4$; $\Delta = 0.05\%$.

where

$$C(U, W) = \frac{1}{2}\left(\frac{\pi}{aW^3}\right)^{1/2}\left[\frac{U}{VK_1(W)}\right]^2 \tag{21}$$

and

$$D(U, W) = \frac{4\Delta W^3}{3aV^2}.$$

Here $K_1(W)$ is the modified Hankel function.

Fig. 8 shows the total pure bending loss as a function of the normalized fibre length for various rates of change of curvature given by Equation 18. As expected, an abrupt change of curvature ($\pi/ab = 0$) produces a constant rate of loss so that the total loss increases linearly from the beginning of the bend. However when the change of curvature is gradual ($\pi/ab > 0$) the rate of loss is small at the beginning of the bend and rises to a fixed value in the region where the bend radius becomes constant.

A comparison between the transition loss and pure bending loss for various rates of change in curvature is shown in Fig. 9 for $L/a = 2100$, $\Delta = 0.0005$ and $V = 2.4$. For an abrupt change of curvature ($\pi/ab = 0$) the pure bending loss exceeds the transition loss at small bend radii (say $R/a \leqslant 12\,000$ which we will call the turning radius). However at large bend radii the transition loss exceeds the pure bending loss and therefore discontinuities, due to changes in curvature, play a significant role in determining fibre curvature losses. With increase in the length of the continuous transition it can be seen that the transition loss decreases considerably compared with the change of pure bending loss and thus the turning radius becomes larger. These results clearly indicate that the pure bend loss also influences the curvature loss in the case of a continuous change of curvature even at large bend radii. The very important conclusion must therefore be drawn that the usual assumption for the calculation of microbending loss, which takes into account only mode conversion, may well not be valid. In fact, as we have shown, both mechanisms contribute to microbending loss, as well as curvature loss, in single-mode fibres.

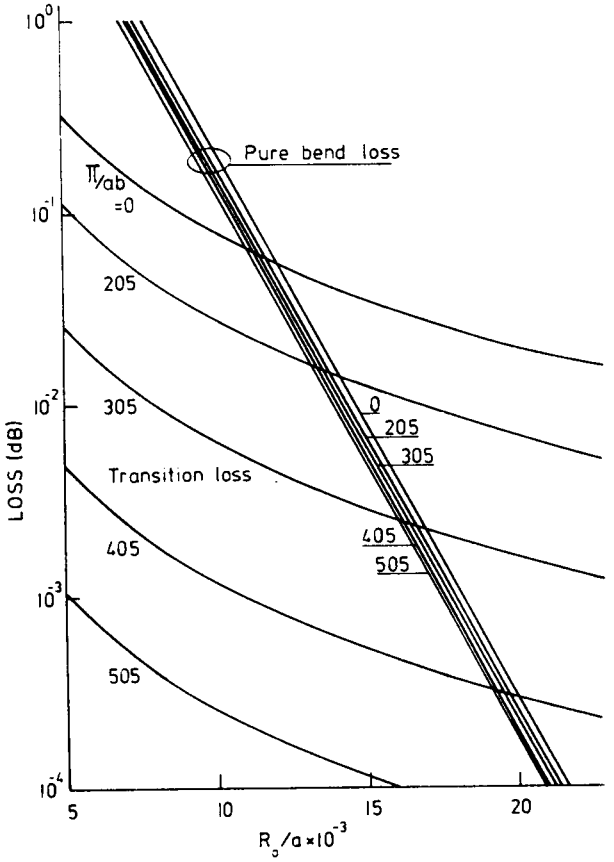

Figure 9 Pure bend loss and transition loss for various rates of change of curvature with L/a = 21 000; V = 2.4; Δ = 0.05%.

4. Microbending loss in a single-mode fibre

In the past the effect of the pure bend component has been neglected in the calculation of microbending loss [9, 10] because it is normally assumed that the radii of curvature involved are large and that mode conversion predominates. However, as indicated in Section 3 above, the transition loss decreases much more rapidly than the pure bend loss as the rate of change of curvature is decreased. It is necessary, therefore, to consider both these effects in detail.

In practice various kinds of non-uniform stress also contribute to the transition loss component, but here we consider only the effect of curvature and assume that the power spectrum adopted takes account of such stresses.

4.1. Transition loss component caused by random deformations

Using Equation 9, the power in the radiation modes, and thus the microbending loss coefficient due to the transition component, of a single-mode fibre having a randomly deformed axis can be obtained by taking the ensemble average of the Fourier spectrum of the distortion function, $F^2(L, X)$, from Equation 10. Thus

$$\alpha_t = \left\langle \frac{P_r}{(L/a)} \right\rangle = 2A(U, W) \int_{-kn_2a}^{kn_2a} B(X) \langle F^2(L, X) \rangle \, dX \tag{22}$$

where $\langle\,\rangle$ denotes the ensemble average and $\langle F^2 \rangle$, the power spectrum of the fibre deformation, is given by

$$\langle F^2 \rangle = \left| \frac{1}{\sqrt{(L/a)}} \int_0^L \int_0^L \left\langle \frac{1}{R(z)R(z')} \right\rangle \exp\left[j(X - X_0) \frac{(z - z')}{a} \right] dz dz' \right|. \tag{23}$$

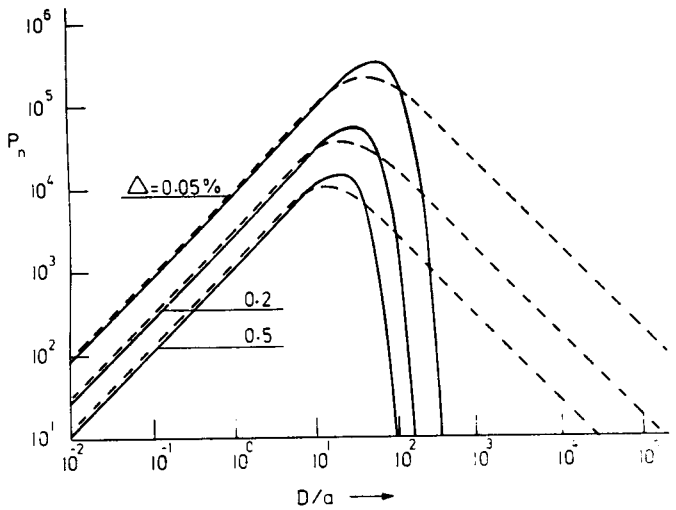

Figure 10 Normalized transition loss P_n as a function of correlation length D for various Δ at $V = 2.4$ for Cases 1 (solid curves) and 2 (dashed).

The autocorrelation function for the ergodic random curvature system is given by

$$S(u) = \left\langle \frac{1}{R(z)R(z+u)} \right\rangle \tag{24}$$

so that from Equation 23 and [19]

$$\langle F^2 \rangle = \int_{-\infty}^{\infty} S(u) \exp\left[j(X - X_0)\frac{u}{a} \right] du \,. \tag{25}$$

Since it is not known what type of correlation function should be attributed to the axis deformations, we consider the two cases

$$\begin{aligned} &\text{(Case 1)}\ S(u) = 2\bar{\sigma}^2 \exp(-u^2/D^2) \\ \text{and} \quad &\text{(Case 2)}\ S(u) = 2\bar{\sigma}^2 \exp(-|u|/D) \end{aligned} \tag{26}$$

where $2\bar{\sigma}^2$ is the variance of $1/R(z)$ and D the correlation length.

Since we assume that $\langle 1/R(z) \rangle = 0$ it follows that $\sqrt{2}\bar{\sigma}$ is the r.m.s. deviation. From Equations 25 and 26, the power spectra are given by

$$\begin{aligned} &\text{(Case 1)}\ \langle F^2 \rangle = 2\sqrt{\pi D}\,\bar{\sigma}^2 \exp\{-[D(X - X_0)/2a]^2\} \\ \text{and} \quad &\text{(Case 2)}\ \langle F^2 \rangle = \frac{4\bar{\sigma}^2}{D}\left\{ \frac{1}{[(X - X_0)/a]^2 + (1/D)^2} \right\}. \end{aligned} \tag{27}$$

Equations 22 and 27 enable the transition loss component of microbending loss in a single-mode fibre to be found. It is convenient to introduce a dimensionless normalized loss, $P_n = P_r/[(\bar{\sigma}a)^2 (L/a)^2]$, given as a function of the normalized correlation length (D/a) in Fig. 10 for various values of Δ. The solid and dotted curves refer to Cases 1 and 2, respectively. It can be seen from Fig. 10 that the loss changes considerably with the correlation length. The curves to the left of the maximum do not depend on the form of the correlation function, but the losses to the right of the maximum do so strongly. The loss also depends on Δ, i.e. the numerical aperture (NA) of the fibre [18], and the effect is particularly significant for larger correlation lengths. A most important result is that the transition microbending loss is a maximum at values of D/a between 15–65, for example, in Case 1 at $D/a = 32$ when $\Delta = 0.2\%$. The maximum values are nearly the same for Case 1 and Case 2.

In order to explain the shape of the curves it is necessary to calculate the normalized power-weighted mean value of the propagation constants of the radiation modes ($X_e = \beta_e a$ in Equation 13). Instead of

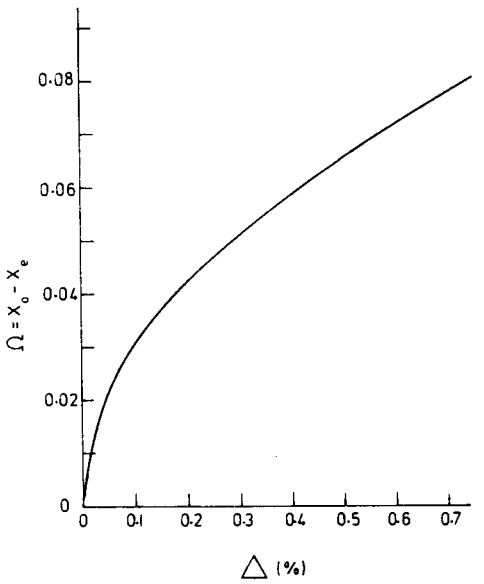

Figure 11 Difference between the normalized propagation constant of the HE_{11} mode and the mean for the radiation modes, at $V = 2.4$, as a function of Δ. The random curvature power spectrum is given by Equation 28.

using Case 1 and Case 2, for convenience (see below) the more general form of the curvature spectrum defined by Olshansky [20] is taken, so that

$$\langle F^2 \rangle = C_0/(\beta - \beta_0)^{4+2p} \tag{28}$$

where p typically has the value 0, 1 or 2, depending upon the nature of the external stress and the fibre diameter, while C_0 is a constant depending upon the correlation length, coupling strength, etc. The transition microbending losses associated with the above power spectrum have been obtained from Equations 22 and 28 as functions of Δ and p. It is found that the losses decrease strongly with increasing Δ. For instance, the ratio of the microbending loss for $\Delta = 0.24\%$ (NA ~ 0.1, $V = 2.4$ and $a \sim 3.8$ μm at $\lambda = 1$ μm) to that for $\Delta = 0.06\%$ (NA ~ 0.05, $V = 2.4$, and $a \sim 7.6$ μm at $\lambda = 1$ μm) is about 10^{-3} for $p = 0$ and 10^{-4} for $p = 1$. It is therefore very important to use as high a numerical aperture as possible in any application of single-mode fibres to long-distance telecommunications.

$X_e = \beta a$ has also been calculated, using Equations 13 and 28, for various values of p as a function of Δ. The difference between the normalized propagation constant of the HE_{11} mode and X_e is denoted by Ω and is shown in Fig. 11. It is found that p has little effect on X_e and Ω so that Fig. 11 can be used, to a good approximation, for most forms of random fibre deformation. This is why the power spectrum of Equation 28 was conveniently taken instead of that for Case 1 or Case 2. Fig. 11 now shows clearly why a fibre of large NA exhibits low values of transition loss. It can be seen that Ω increases with Δ and therefore coupling from the HE_{11} mode to the radiation modes becomes progressively weaker with increasing Δ.

The above analysis, although essential for a full study of the transition loss caused by microbends, is rather complex and it is sometimes useful to seek a simpler result which can be used for approximate calculations. If the heuristic approach suggested at the end of Section 2.2.1 is followed then it might be expected that the radiation loss would be a maximum when the correlation length D is related to the difference in phase constants of the HE_{11} and quasi-radiation modes by an equation of the form

$$D_m/a = 2\pi/m(X_0 - X_e) .$$

Choosing (arbitrarily) a value of $m = 4$ so that

$$D_m/a = \pi/2(X_0 - X_e) \tag{29}$$

gives good agreement to the more rigorous result, as indicated by Table I, calculated for Case 1.

TABLE I Normalized correlation length D_m/a giving maximum radiation loss predicted by (a) Equation 29 and (b) rigorous calculation

	Δ (%)		
Calculation	0.05	0.2	0.5
rigorous	65	35	20
Equation 29	73	37	23

It can be seen that the two sets of values are in reasonable agreement, confirming that Equation 29 gives a good approximation to D_m/a and may be used for the prediction of maximum microbending transition loss.

Finally, a few numerical calculations will be given. The maximum microbending transition loss for a fibre with $V = 2.4$, $\Delta = 0.2\%$ and $\lambda = 1$ μm are 5.5 dB m^{-1} and 5.5 × 10^{-2} dB m^{-1} for $\bar{\sigma}a = 10^{-5}$ and 10^{-6}, respectively. The correlation length in these cases is 0.145 mm.

4.2. Pure bend loss component caused by random deformations

It is difficult to deduce from Equation 20 the pure bend loss component caused by random deformations of the fibre axis. However if we assume a probability density function which describes the probability that the random deformations will assume a value within some defined range, then it is possible to estimate the mean value. Several types of probability density function can be considered, but we will use the common exponential function defined by

$$p(1/R) = \frac{1}{2\bar{\sigma}} \exp\left(-\frac{|1/R|}{\bar{\sigma}}\right). \tag{30}$$

The mean square value of $1/R$ is given by

$$\psi^2 = \frac{1}{2\bar{\sigma}} \int_{-\infty}^{\infty} \frac{1}{R^2} \exp\left(-\frac{|1/R|}{\bar{\sigma}}\right) \mathrm{d}(1/R) = 2\bar{\sigma}^2 \tag{31}$$

which is the same as that derived in the previous section (see Equation 26). By taking the mean value of α_b in Equation 20 and introducing Equation 30, we get

$$\langle\alpha_b\rangle = \frac{LC(U, W)}{\bar{\sigma}} \int_0^{\infty} \left(\frac{1}{R}\right)^{1/2} \exp\left[-\frac{(1/R)}{\bar{\sigma}} - \frac{D(U, W)}{(1/R)}\right] \mathrm{d}(1/R). \tag{32}$$

With the help of the equation in Appendix B it can be shown that $\langle\alpha_b\rangle$ is given by

$$\frac{\langle\alpha_b\rangle}{L} = [\pi D(U, W)]^{1/2} C(U, W) \left[1 + \tfrac{1}{2}(\bar{\sigma}/D)^{1/2}\right] \exp\left[-2(D/\bar{\sigma})^{1/2}\right]. \tag{33}$$

Fig. 12 shows the normalized random bending loss $\langle\alpha_b/(L/a)\rangle$ as a function of the inverse r.m.s. deviation for various Δ at $V = 2.4$. It is found that the bending loss depends strongly on $\bar{\sigma}a$ and Δ. In particular, for $(\bar{\sigma}a)^{-1} > 3 \times 10^3$ the loss decreases very rapidly. Therefore in practice a fibre having a large Δ must be used and the cabling process must be carefully controlled in order to keep $\bar{\sigma}a$ small. To take a numerical example, if $\Delta = 0.2\%$ and $\lambda = 1$ μm then the pure bend losses are 2.6 dB m^{-1} and 0.015 dB m^{-1} for $\bar{\sigma}^{-1} = 58$ mm and 124 mm, respectively. In order to keep the loss below 1 dB km^{-1} then $\bar{\sigma}^{-1}$ has to be made larger than 200 mm.

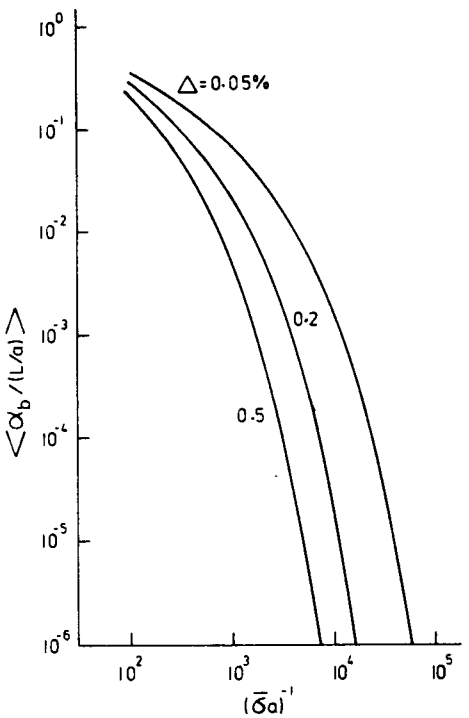

Figure 12 Average pure bend loss due to random curvature as a function of the inverse r.m.s. deviation of $1/R$ for $V = 2.4$.

4.3. Comparison between the transition loss and pure bend loss components of microbending

Finally it is interesting to make a comparison between the magnitudes of the transition and pure bend loss components as represented by Figs. 10 and 12. In fact it is difficult to compare them accurately because they depend strongly on the shapes of the correlation and probability density functions. However, it is necessary to make as good an estimate as possible of their relative effects.

Thus the ratio of the transition loss for the correlation length of Case 1 of Equation 26 to the pure bend loss, as a function of the correlation length, is shown in Fig. 13 for various r.m.s. deviations of $1/R(z)$ with $V = 2.4$ and $\Delta = 0.02\%$. It is found that the maximum of the transition loss is always larger than the pure bend loss, but for large correlation lengths (generally $D/a > 5 \times 10^2$) and, in addition, for small correlation lengths [say $D/a < 9 \times 10^{-1}$ at $(\bar{\sigma}a)^{-1} = 10^4$] the pure bend loss exceeds the transition loss. In a typical practical situation the r.m.s. deviation of $1/R(z)$ is very small and, moreover, the correlation length is large compared with the fibre diameter, so that the shape of the correlation function has to be chosen carefully and both loss effects have to be taken into account.

5. Conclusions

In this paper a theoretical study has been made of the transition loss and the pure bend loss which can arise in a single-mode fibre containing random bends.

A modified mode coupling theory has been derived which can be applied to the general problems connected with curved fibres and has been used for the first time to predict transition losses. This modified theory is based on the notion that the propagation characteristics of a curved fibre are equivalent to those of a straight fibre for which the influence of the fibre curvature is taken into account by introducing an effective refractive-index profile. The resulting coupling coefficient between the HE_{11} mode and the radiation modes differ from that of Marcuse [14] in that our coefficient contains a $1/(\beta_0^2 - \beta^2)^2$ term. This term has a very large influence on the calculated radiation loss, especially when $\beta_0 \sim \beta$, where β_0, β are the propagation constants of the HE_{11} mode and the radiation modes, respectively.

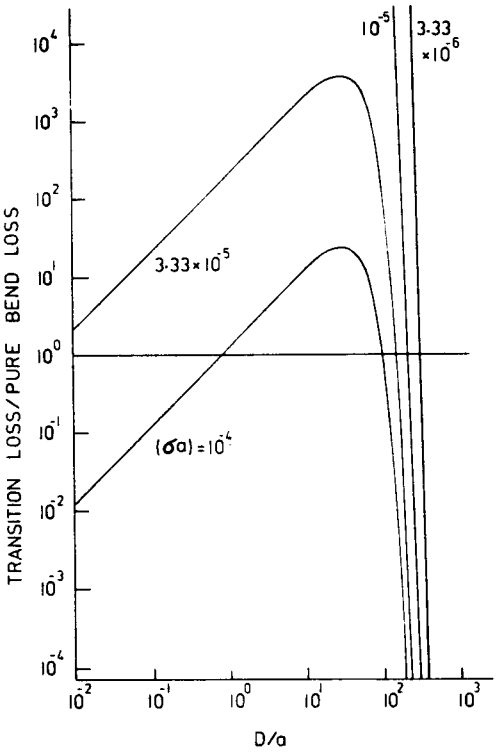

Figure 13 Ratio of transition loss to pure bend loss as a function of correlation length for various values of $\bar{\sigma a}$ and $\Delta = 0.2\%$. The transition loss assumes the correlation function of Case 1 and the pure bend loss is for the Gaussian probability density function.

By using this modified mode coupling theory, the loss induced at a transition between straight and curved sections of fibre has been calculated and it is found that the radiated power is oscillatory at the beginning of the bend, as has been observed experimentally. This implies the existence of an exchange of power between the HE_{11} mode and the radiation modes. In those (periodic) regions where the power flow is predominantly out of the HE_{11} mode, the radiation modes all have almost the same propagation constant, so that the radiation emitted from the curved fibre resembles discrete beams. With increase of distance along the curved axis the radiated power asymptotically approaches a constant level, having a magnitude which is almost the same as that obtained previously by Miyagi and Yip [4] and ourselves [7].

Generally speaking, the propagation constants of most of the radiation modes lie within a small range so that, for small lengths of curved fibre, they can be represented by a single quasi-guided (β_e) mode, where β_e is the power-weighted average propagation constant of the radiation modes. The problem can thus be simplified to one of coupling between only two modes. In terms of β_e the periodic length corresponding to the separation between the discrete radiation rays is given, to a good approximation by $2\pi/(\beta_0 - \beta_e)a$, where a is the radius of the fibre. This expression is in good agreement with experimental measurements.

A continuous change of curvature between the straight and constantly-curved fibres reduces considerably the transition loss as well as the pure bend loss. It is found that for longer lengths of continuous region the radius of curvature at which the pure bending loss exceeds the transition loss increases.

The contributions of the transition and pure bend loss components to microbending have also been analysed, using a Gaussian type of autocorrelation function and a probability density function. The transition loss component has a maximum at a certain correlation length given approximately by $\pi/2(\beta_0 - \beta_e)$. The power-weighted average propagation constant β_e for fibre bending has been found as a function of the relative refractive-index difference. The microbending loss depends strongly on the shape of the correlation function in the region of large correlation length. The maximum transition loss

component is normally larger than the average pure-bend loss component but for large correlation length, the latter predominates. It is always necessary, therefore, to take both these losses into account in the prediction of the microbending loss.

Appendix

A. Let functions $Z_n(x)$ and $Z_m^*(y)$ be cylindrical functions

$$\int Z_0(kr)Z_1^*(\alpha r)r^2\,dr = \frac{2\alpha r}{(\alpha^2-k^2)^2}[\alpha Z_0(kr)Z_1^*(\alpha r) - kZ_1(kr)Z_0^*(\alpha r)] - \frac{r^2}{(\alpha^2-k^2)^2}[\alpha Z_0(kr)Z_0^*(\alpha r) + kZ_1(kr)Z_1^*(\alpha r)].$$

B. $K_\mu(z)$ is the modified Bessel function of order μ

$$\int_0^\infty x^{\mu-1}\exp(-Bx^n - Ax^{-n})\,dx = \frac{2}{n}\left(\frac{A}{B}\right)^{(\mu/2n)} K_{\mu/p}[2\sqrt{(AB)}] \qquad \text{for } R_e(B)>0 \text{ and } R_e(A)>0$$

and

$$K_{3/2}(z) = \left(\frac{\pi}{2z}\right)^{1/2}(1+z^{-1})\,e^{-z}.$$

Acknowledgements

We wish to thank Dr D. N. Payne for stimulating discussions, Dr R. A. Sammut for useful comments and the Science Research Council for financial support. Grateful acknowledgement is also made to the Pirelli General Cable Company Ltd for the award of a research fellowship.

References

1. L. LEWIN, *IEEE Trans. Microwave Theory Tech.* **MTT-22** (1974) 121–29.
2. A. W. SNYDER, I. WHITE and D. J. MITCHELL, *Electron. Lett.* **11** (1975) 332–33.
3. D. MARCUSE, *J. Opt. Soc. Amer.* **66** (1976) 311–20.
4. M. MIYAGI and G. L. YIP, *Opt. Quant. Elect.* **9** (1975) 51–60.
5. W. A. GAMBLING and H. MATSUMURA, *Trans. Inst. Electron. Commn. Engrs. Japan* **E61** (1978) 196–201.
6. W. A. GAMBLING, H. MATSUMURA and R. A. SAMMUT, *Electron. Lett.* **13** (1977) 695–97.
7. W. A. GAMBLING, H. MATSUMURA and C. M. RAGDALE, *ibid* **14** (1978) 130–32.
8. W. A. GAMBLING, H. MATSUMURA, C. M. RAGDALE and R. A. SAMMUT, *Microwaves, Opt. Acoust.* **3** (1978) 134–40.
9. D. MARCUSE, *Bell Syst. Tech. J.* **55** (1976) 937–55.
10. K. PETERMANN, *Opt. Quant. Elect.* **9** (1977) 167–75.
11. W. A. GAMBLING, D. N. PAYNE and H. MATSUMURA, *Electron. Lett.* **12** (1976) 567–69.
12. R. A. SAMMUT, *ibid* **13** (1977) 418–19.
13. C. G. SOMEDA, *ibid* **13** (1977) 712–13.
14. D. MARCUSE, 'Theory of Dielectric Optical Waveguides' (Academic Press, New York, 1974).
15. W. A. GAMBLING, D. N. PAYNE and H. MATSUMURA, *Proceedings of AGARD Conference on Electromagnetic Wave Propagation involving Irregular Surfaces and Inhomogeneous Media*, The Hague (March 1974) 12.1–12.16.
16. H. F. TAYLOR, *Appl. Opt.* **13** (1974) 642–47.
17. E. A. J. MARCATILI and S. E. MILLER, *Bell Syst. Tech. J.* **48** (1969) 2161–2187.
18. W. A. GAMBLING and H. MATSUMURA, *Electron. Lett.* **13** (1977) 691–93.
19. D. MARCUSE, 'Light Transmission Optics' (Van Nostrand Reinhold Co, New York, 1972).
20. R. OLSHANSKY, *Appl. Opt.* **14** (1975) 925–45.